Maciej CHOJOWSKI

DOI: 10.15199/48.2025.05.38

Exploring bandwidth requirements for high-speed measurements in power electronics

Badanie wymagań pasma przenoszenia dla szybkich pomiarów w elektronice mocy

***Abstract**. The article proposes a different bandwidth and rise time product factor for fast transient voltage measurement. The article does not focus on the method of current measurement, but on the general requirements for high-frequency measurements in power electronics. The theoretical square-wave voltage signal was generated using Fourier series to determine the relationship be-tween rising time and bandwidth. The article presents analytical considerations regarding the proposed method. In addition to the slope measurement requirement, the ringing effect was also described for extracting frequency in a simplified half-bridge circuit during a double-pulse test. The bandwidth of the oscilloscope and voltage probe was calculated for various setup types and compared. The article highlights the problem of mismatch between the oscilloscope and probe bandwidth and experimentally confirms the bandwidth requirements for a commercial GaN transistor. Overall, the article covers a comprehensive analysis of the bandwidth and rising time relation for fast transient voltage measurement, including theoretical considerations, experimental validations, and discussions on potential issues such as bandwidth mismatch. Ogólnie rzecz biorąc, artykuł zawiera kompleksową analizę związku między pasmem a czasem narastania dla pomiaru szybkich transjentowych napięć, w tym rozważania teoretyczne, walidacje eksperymentalne oraz dyskusje na temat potencjalnych problemów, takich jak niedopasowanie pasma.*

***Streszczenie.** Artykuł ten proponuje inny współczynnik produktu pasma i czasu narastania dla szybkiego pomiaru napięcia transientnego. Artykuł nie koncentruje się na metodzie pomiaru prądu, ale na ogólnych wymaganiach dotyczących pomiarów wysokoczęstotliwościowych w elektronice mocy. Teoretyczny sygnał napięciowy prostokątny został wygenerowany przy użyciu szeregów Fouriera w celu określenia związku między czasem narastania a pasmem. Artykuł przedstawia analityczne rozważania dotyczące proponowanej metody. Oprócz wymogu pomiaru nachylenia, opisano również efekt dzwonienia w celu wydobycia częstotliwości w uproszczonym obwodzie półmostkowym podczas testu podwójnego impulsu. Pasmo oscyloskopu i sondy napięciowej zostało obliczone dla różnych typów układów i porównane. Artykuł podkreśla problem niedopasowania między pasmem oscyloskopu a sondy oraz eksperymentalnie potwierdza wymagania dotyczące pasma dla komercyjnego tranzystora GaN. Ogólnie rzecz biorąc, artykuł zawiera kompleksową analizę związku między pasmem a czasem narastania dla pomiaru szybkich transjentowych napięć, w tym rozważania teoretyczne, walidacje eksperymentalne oraz dyskusje na temat potencjalnych problemów, takich jak niedopasowanie pasma.*

Keywords: bandwidth, high-speed measurements, high-speed measurements
Słowa kluczowe: pasmo, pomiary wysokiej prędkości, pomiary wysokiej prędkości

Introduction

New material based power transistors designed for power electronics applications, such as Gallium Nitride (GaN) and Silicon Carbide (SiC) transistors, present advantages including enhanced efficiency, quicker switching times, and a reduced package size in comparison to their equivalent silicon (Si) counterparts [1–4]. The switching speed of Wide-bandgap semiconductors (WBG) switches can be up to ten times faster than a typical silicon field effect transistor (FET) [1], [4], [5]. Unfortunately, as of now, commercial GaN transistors for higher voltage classes than modern SiC transistors do not exist [6]. Regarding conduction loss, the on-state resistance (Ron) plays a crucial role, while switching loss occurs during the turn-on and turn-off phases of the devices [7–9]. GaN switches demonstrate a lower specific on-resistance lower limit, faster turn--on/off time, and lower parasitic capacitance compared to Si FETs. These characteristics enable GaN switches to support higher switching frequencies [5], [10–12]. Consequently, GaN switches serve as an excellent alternative for designing more efficient power electronics converters [1–5], [7], [9–12]. The fast transient response of Wide-Bandgap (WBG) semiconductors requires a high-bandwidth measurement setup in the laboratory. Bandwidth and rise time are fundamental concepts in signal measurement, for example, during the calculation of switching losses [13]. On the other hand, rise time quantifies the duration required for a signal to transition from a specified low value to a specified high value, serving as a metric for system speed or response time [13]. The interplay between rise time and bandwidth is governed by the formula: = 0.35, where 0.35 is a constant representing the time taken for a signal to rise from 10% to 90% of its final value – a widely accepted definition of rise time. This constant factor of 0.35 is typically approximated for a first-order inertia system and commonly applied in measurement techniques and many articles [14–17]. However, practical measurements extend beyond the scope of first-order inertia systems, necessitating the determination of this value for various signal types [13]. In hard-switching power electronics, for instance, measured voltage and current often exhibit quasi-square shapes, deviating from sinusoidal forms [7–9]. Only resonant converters in power electronics can produce quasi-sinusoidal current or voltage. Understanding the nuanced relationship between bandwidth and rise time is paramount in the design and analysis of measurement equipment for calculating transistor switching losses [18–21].

In the second chapter of the article, a theoretical square signal with a rapid rise time and intentional overshoot was determined. A Fourier series was used as a design tool, providing a mathematical foundation for achieving the desired signal characteristics and extracting important information about the relationship between bandwidth and rising time. The product for a quasi-square wave was the main focus of the second chapter. Chapter four simplified and presented all theoretical aspects of Wide-Bandgap (WBG) semiconductors during switching. All important aspects were simplified to demonstrate frequency requirements for measurement purposes. Chapter five discussed issues related to bandwidth mismatch with a digital oscilloscope and probe in a general context, which is significant because both elements are always connected during measurements. Lastly, chapter six presented practical results of voltage measurements in the double-pulse test (DPT) circuit [20–22], providing detailed descriptions and confirming previously determined bandwidth requirements.

Theoretical bandwidth requirement for wide-bandgap semiconductors measurements

In hard switching powered electronic converter both of the transistor current and voltage are quasi square type. When we consider a square wave function f (t) in time t of period T:

(1) $$f(t) = 2\left[H\left(\frac{2t}{T}\right) - H\left(\frac{2t}{T} - 1\right)\right] - 1$$

Where is the Heaviside step function. The f (t) is an odd function and the Fourier coefficients are given by:

(2) $$A_0 = A_n = 0 \wedge B_0 = \frac{2}{T}\int_{t_o}^{T+t_o} f(t)\sin sin\left(\frac{2n\pi t}{T}\right)dt$$

The Fourier series is therefore:

(3) $$f(t)_{SQUARE} = \frac{4}{n\pi}\sum_{n=1,3,5,...}^{inf}\frac{1}{n}sin(\frac{2n\pi t}{T})$$

The squared signal can be reasonably approximated within the range of 1 to 50 harmonics, and the rise time (10% to 90%) for each signal can be accurately measured. The presented Figure 1 illustrates the results, showcasing the calculated bandwidth of generated waveform based on only equation (3). The fitted curve in figure 1 was made by equation (4).

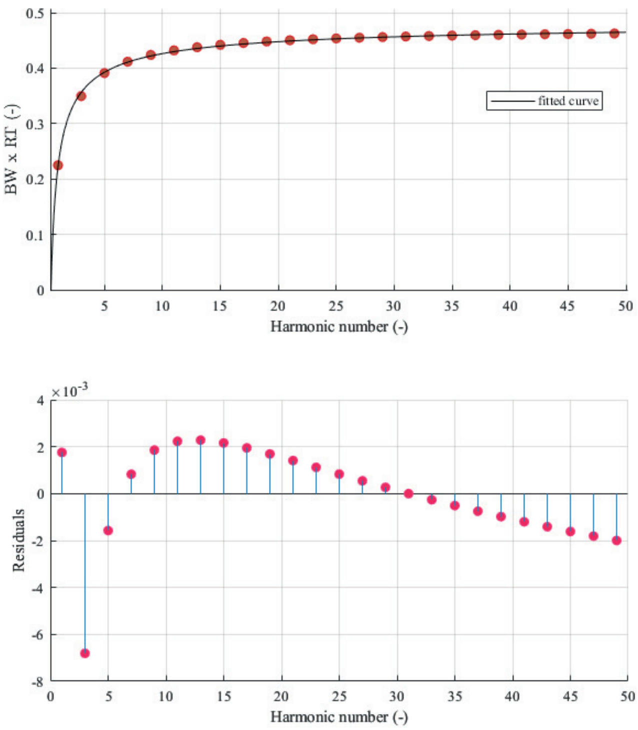

Fig. 1. Product of bandwidth and rise time of the signal vs Harmonic number in generated waveform and fitting residuals.

Bandwidth of the highest harmonics and their corresponding rise times has been approximated with following fit function:

(4) $$x_{fit-BWxRT} = ax^b + c$$

A approximation was achieved, with an R^2 value of 0.998, using a power function curve (4) – R^2 defined by following form: $R^2 = 1 - \Sigma (y_i - \hat{y}_i)^2 / \Sigma (y_i - \bar{y})^2$. Specifically, for the signal with 50 harmonics, the fitted curve matched the calculated rise time with a approximation constant c = 0,47. And finally the product of BW and rise time is defined by:

(5) $$BW \cdot t_{r/f} \approx 0.47$$

A relation product for various odd harmonic number in square waveform were listed in Table I.

Table 1. Bandwidth and rise time product

Harm. No.	1	3	5	9	30	50	1000
$BW \cdot t_r$	0.22	0.35	0.39	0.42	0.46	0.46	0.47

The value for 3 harmonics in signal is close to first order inertia system. In summary, the constants for signals with more than 1000 harmonics consistently surpass, representing 134% of the commonly used value (0.35). Relying solely on the value of a first-order inertia system highlights a significant deviation from conventional assumptions, underscoring the importance of taking into account higher harmonics in the signal.

Simplify analysis of switching behavior of power electronics transistor

When measuring current and voltage for power transistors, a frequent challenge arises in calculating switching losses. The Double Pulse Test (DPT) is widely employed test circuit in power electronics to assess the switching characteristics and observe switching performance of Wide-Bandgap (WBG) semiconductors. The GaN transistor, for instance, can achieve on/off transitions within a few nanoseconds [1], [2], [8], [17], [22]. That means the measurement system bandwidth requirement of the signal based rise/fall edge on in the slope Is calculated by equation (5).

The measured rise time or fall time from 10% to 90% of voltage steady state value. The DPT equivalent circuit of the switching transient is shown in the Figure 2. The circuit is

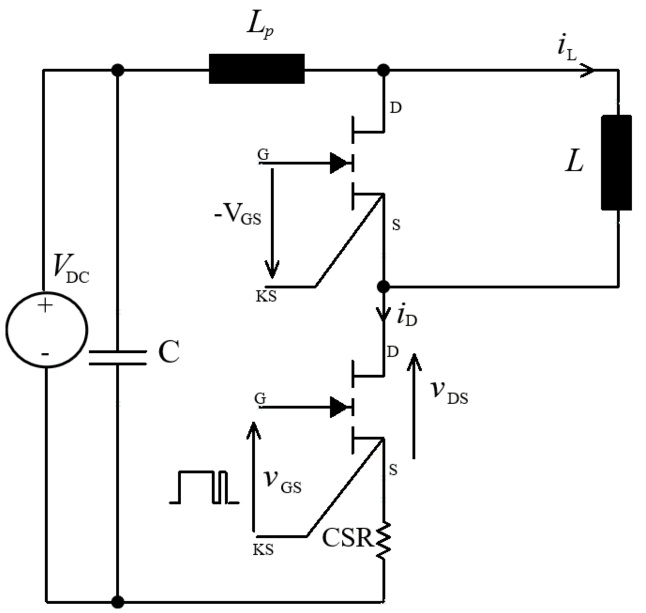

Fig. 2. A double pulse test circuit with GaN transistors and current shunt resistor CSR.

connected to DC power supply with parasitic power loop inductance L_p. The inductance represent the whole sum of all power loop inductance connected in series. In practical circuit it will be all traces/wires, transistor package inductance, internal inductance of elements and additional inductance of current sensor in circuit [23]. Practically, the parasitic inductance cannot be completely decoupled by main C capacitor due to the package of power device and interconnections of the PCB layout.

The next Figure 3 present a lower transistor during switching process. When the transistor is turn on than the channel model can be represent by open circuit, but when the transistor will be turned on, than the resistor will represent a transistor channel. The FET channel of the power transistor can be also represented by controlled current source in transient mode between ON and OFF. Parasitic capacitances of the transistor (C_{DS}, C_{GS}, C_{GD}) where also presents in the figure 3. In this circuit, the influence of the gate stage loop was ignored since it plays a less significant role in the ringing stage. The upper device is represented as a diode with its junction capacitance CJ. Note the diode representation is technically not true for GaN HEMT since they do not have the same parasitic diode as MOSFETs, but is still used because their reverse conduction behavior is similar to a diode.

The figure 4a shows simplified circuit during turn-on with output capacitance C_J and parasitic power loop inductance. When upper and lower transistors are similar it can be replaced by output capacitance C_{OSS}. The $R_{ds\ (on)}$ represent the on state resistance of the DUT and Rp the parasitic resistance of all elements in power loop. The resistance can be summarized to stray resistance RS of the power circuit. Both circuit in the Figure 4a and Figure 4b will be similar when both transistors (high side and low side) will be the same [24]. In must be also stated that the simplified model can be used only to extract oscillation effect and it can not be used to model all switching effect in the power FET. The schematic diagrams are intentionally simplified to illustrate the switching behavior of the FET. Specifically, the output capacitance Coss is depicted separately for conceptual clarity, although in practice it is intrinsically connected in parallel with the FET's drain-source path.

Turn-on Oscillation based on Figure 4c, the following relationship between VDC and ID can be presented by transfer function:

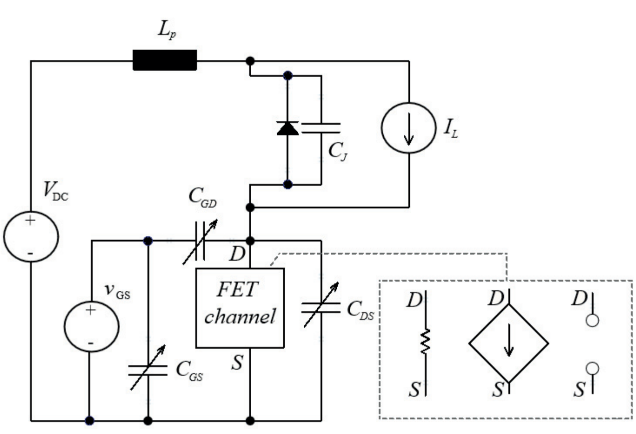

Fig. 3. A double pulse test circuit with lower GaN transistor during switching – equivalent circuit.

(6) $$\frac{I_D(s)}{V_{DC}(s)} = \frac{C_J s}{(L_p C_J)s^2 + (R_s C_J)s + 1}$$

Turn-off (Figure 4d) Oscillation similarly as (6), the relationship between V_{DC} and I_{DS} in the ringing stage during turn-off can be expressed as:

(7) $$\frac{V_{DS}(s)}{V_{DC}(s)} = \frac{1}{(L_p C_{OSS})s^2 + (R_s C_{OSS})s + 1}$$

When the stray resistance $R_S \approx 0$ is small and $C_J = C_{OSS}$ than the oscillation frequency is similar for turn-on and turn-off and given by (defined voltage ringing oscillation):

(8) $$f_{loop} \triangleq \frac{1}{2\pi\sqrt{L_p C_{OSS}}}$$

In practical GaN power switch the output capacitance in most cases is from few to few hundred pF and the power loop inductance in properly designed topology does not exceed several or several tens of nH. Based on equation (5) and (8) the general requirements of bandwidth for the modern power transistor can be stated:

(9) $$f > \left(\frac{1}{2\pi\sqrt{L_p C_{OSS}}}, \frac{0.47}{(t_r, t_f)}\right)$$

Bandwidth of digital storage oscilloscope and voltage probe

Authors should discuss the results and how they can be interpreted from the perspective of previous studies and of the working hypotheses. The findings and their implications should be discussed in the broadest context possible. Future research directions may also be highlighted.

In reference to Figure 5, it is evident that the circuit features a notable input resistance, denoted as R_{in}, measuring 9 MΩ.

This resistance is with a 3.9 pF bypass capacitance in parallel and is terminated by an impedance of 1 MΩ at the oscilloscope, denoted as R_{osc}. The inductance of the ground loop, designated as L_{ground}, is contingent upon the type of ground lead employed. Specifically, utilizing a 6-inch ground lead with the high-bandwidth (1 GHz) passive probe TPP1000 results in

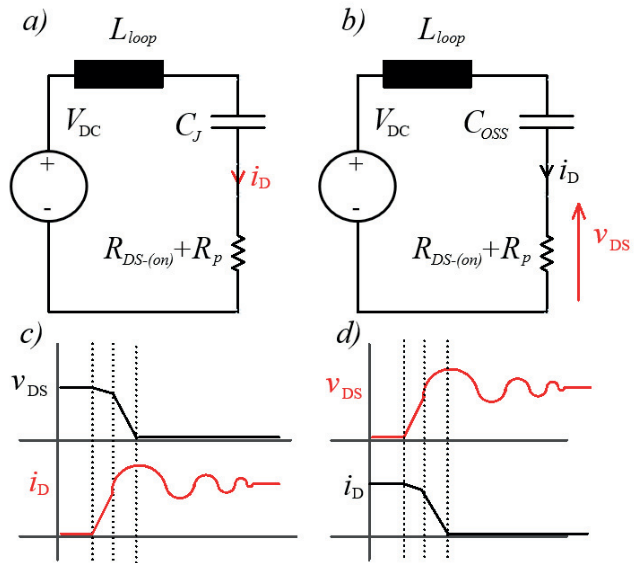

Fig. 4. Simplified circuit for a) turn ON and b) turn OFF. Theoretical visualization of quasi sinusoidal ringing effect during c) ON and d) OFF transistor transient state.

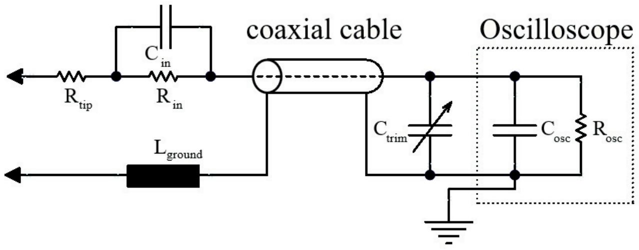

Fig. 5. An expanded voltage passive probe with coaxial cable and oscilloscope.

a grounding inductance of 150 nH, whereas employing a short a half inch spring lead reduces the inductance to 10 nH. It is noteworthy that variations in ground inductance lead to changes in the self-resonant frequency of the probe, ranging from 208 MHz to 806 MHz. Consequently, it is discerned that employing lengthy grounding cables is ill-suited for high-speed measurements. Further-more, the final bandwidth is influenced by factors such as the shape, relative permittivity, and relative permeability of the probe coaxial cable. It is imperative to highlight that the probe cable differs significantly from conventional coaxial cables, characterized by its status as a lossy coaxial cable. A comparative analysis between a 3 ft length of the probe cable and a 3 ft length of standard BNC/SMA coaxial cable reveals that the latter exhibits relatively low losses compared to the highly attenuating probe cable. Although the resistance of the probe cable can vary from 70 Ω/ft to 300 Ω/ft, pertinent parameters are not provided by manufacturers. Consequently, the substantial resistance in the probe cable effectively attenuates all high-frequency components.

The probe, specifically the Tektronix TPP1000 with a bandwidth of 1 GHz, in con-junction with the Digital Storage Oscilloscope (DSO), notably the MDO3104 also boasting a bandwidth of 1 GHz, has undergone simulation using SPICE software. This simulation aimed to assess the frequency response of the measurement system, as illustrated in Figure 6, against the parameters outlined in Fig 6. Gain and phase response of passive probe with DSO–based on parameters from Table 2.

Based on the simulation results, the Bode plots depict varying values of the system bandwidth for the -3dB point. The bandwidth appears to be approximately 690 MHz, indicating

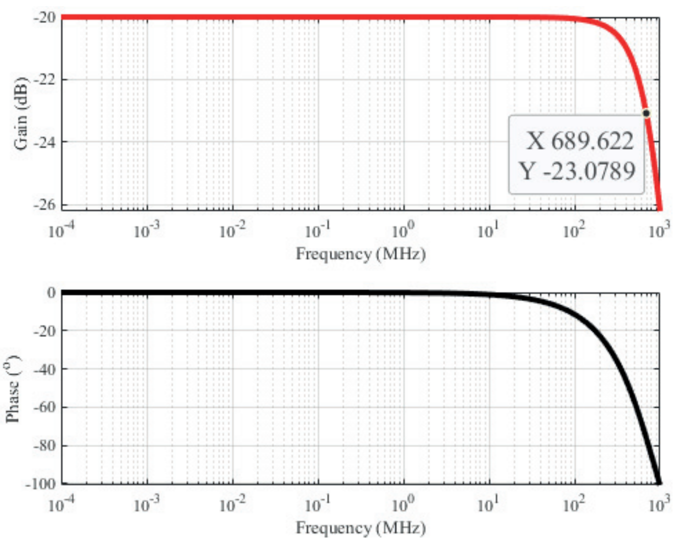

Fig. 6. Gain and phase response of passive probe with DSO – based on parameters from table II.

Table 2. Measurement system parameters.

Parameter	Symbol	Value	Unit
Probe tip resistance	R_{tip}	1.0	Ω
Probe input resistance	R_{in}	9.0	MΩ
Probe input capacitance	C_{in}	3.9	pF
Probe ground loop inductance	L_{groud}	10.0	nH
Coaxial cable resistance	R_{cable}	90.0	Ω
Coaxial cable capacitance	C_{cable}	25.0	pF
Probe compensation adjustment	C_{trim}	7.0	pF
Oscilloscope resistance	R_{osc}	1.0	MΩ
Oscilloscope capacitance	C_{osc}	3.1	pF

that the determination of the system bandwidth must be conducted independently. While the simulation results can offer an accurate bandwidth value, acquiring all parameters from Figure 5 and additional information regarding the coaxial cable is essential. The –3dB value is susceptible to change with coaxial cable resistance, which is often challenging to obtain from datasheets. Furthermore, it is necessary to compensate the simulated probe with adjustable capacitance C_{trim}.

To avoid complex simulation of measurement system, the system bandwidth for passive probe and DSO can be calculated by:

$$W_S = \frac{1}{\sqrt{\frac{1}{BW^2_{scope}} + \frac{1}{BW^2_{probe}}}} \tag{11}$$

The table 3 lists example system bandwidth for different passive probe. Based on Table 3 for similar bandwidth which is 1 GHz in this example, the system bandwidth is much lower and equal 707.11 MHz. In general when the DSO bandwidth is five time bigger than probe bandwidth than the probe bandwidth will dominate.

This example (Table 3) and following conclusions can be also useful for different frequency range. More over, to accurately measure power with an oscilloscope, it is important to use hi-resolution mode to achieve maximal available resolution (for example in MDO3104 it is 11 bits) and compensate probe before measurements.

Table 3. Calculated measurement system bandwidth for various probes and one scope (1 GHz).

Probe name	Probe BW (MHz)	System BW (MHz)
Tektronix TPP1000	1000	707.11
Tektronix TEK P6139A	500	447.21
Tektronix TPP0201	200	196.12
Testec TT-LF312	150	148.34
Agilent P6100	100	99.50
Hantek PP80B	80	79.75
GWinstec GTP-070B-4	70	69.83

Bandwidth of digital storage oscilloscope and voltage probe

This section is not mandatory but can be added to the manuscript if the discussion is unusually long or complex.

A DPT topology has been assembled on a GS66508T GaN EHEMT Daughter Board and GS665MB Evaluation Platform. The board contains two GaN E-HEMT GS66508B power MOSFETs with a 650 V breakdown voltage and 50 mΩ on state channel resistance [24]. The main inductance L was constructed FINEMET inductor (L = 90 μH). The utilized experimental set-up is shown in Figure 7.

Base on datasheet the rising time and falling time of GS66508B are 3.7 ns and 5.2 ns, respectively [25]. Both value ere measured for drain-source voltage equal to 400 V but for lower voltage the time can be even shorter. The lowest measured value was 2.9 ns. The rising/falling time requirement for the Bandwidth is:

(12) $$BW = \frac{0.47}{min(t_r,t_f)} = \frac{0.47}{2.9 \cdot 10^{-9}} = 162.08\ MHz$$

And the ringing requirement for GS66508B (COSS = 65 pF) and extracted inductance of power loop Lp = 11 nH of the parasitic elements is:

(13) $$f_{loop} = \frac{1}{2\pi\sqrt{L_p C_{OSS}}} = \frac{1}{2\pi\sqrt{11 \cdot 65 \cdot 10^{-21}}} = 188.22\ MHz$$

The final requirement for the measurement system bandwidth, based on equation (10), is a higher frequency value of 188.22 MHz. Figure 8 presents the measured drain-source voltage in the DPT circuit using a passive voltage probe. Probe ground springs were utilized to minimize ground lead inductance. Before the test, the passive probe was compensated. The MDO3104 oscilloscope, equipped with a 1 GHz band and a 10 million points record length with a 5 GS/s sampling rate, was employed during the tests [26]. The responses from all voltage probes were compared with the results obtained using the Tek-tronix 1 GHz TPP1000 probe [27]. Additional tests involving voltage measurements on the same board, oscilloscope, and setup were conducted using lower bandwidth passive probes. The results were compared to confirm the bandwidth requirements for high-speed measurements.

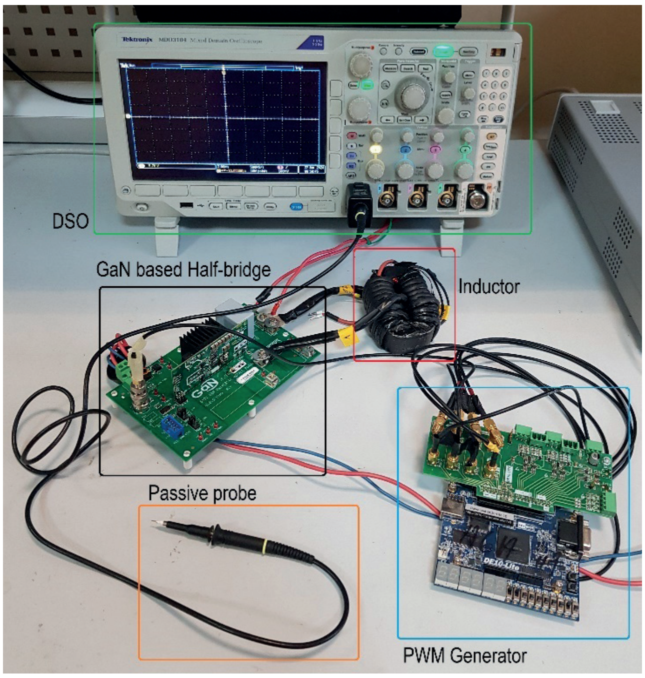

Fig. 7. Laboratory setup for voltage measurement in DPT.

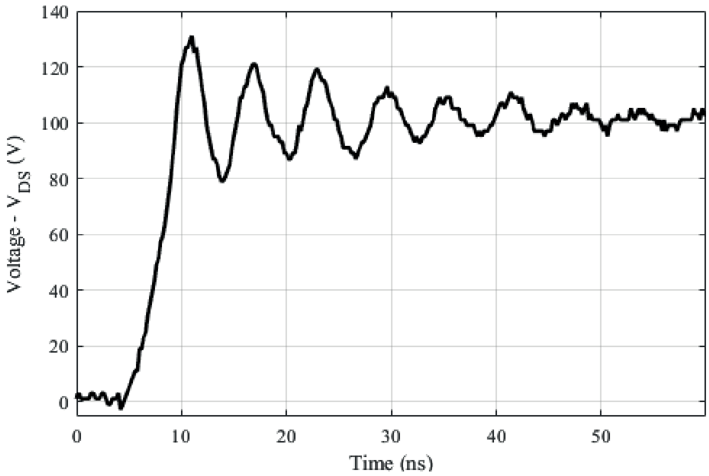

Fig. 8. Measured drain-source voltage within the double pulse test setup, with the DC link voltage set at 100 V.

The Integral of the Square of the Error (ISE) have been calculated for various type of probes (Figure 9) and the reference value was chosen a voltage measured by highest bandwidth probe (1 GHz). ISE was calculated by:

(14) $$ISE = \int e^2(t)\, dt$$

The figure 10 shows rising time error for various probe with different bandwidth. The chosen ISE criteria tends to prioritize minimizing large errors over small errors due to the squaring of error values. Based on result the ISE rise significantly when bandwidth of the probe is small. The theoretical required bandwidth was 188.22 MHz and based on Figure 9 the ISE remain below 2500 V2s and after 175 MHz the error rise faster. When we consider rising time the error is lower

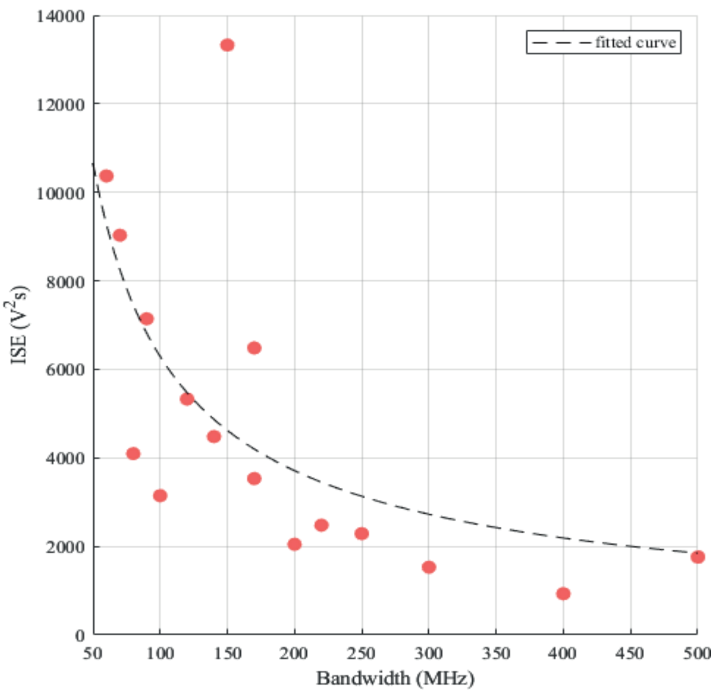

Fig. 9. Integral of the Square of the Error factor vs various probe bandwidth.

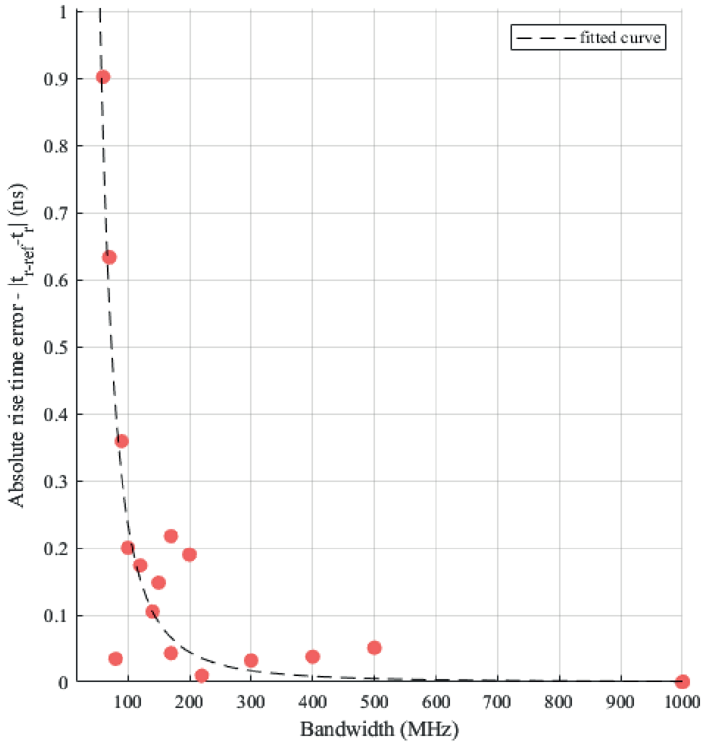

Fig. 10. Rising time mismatch (error value) for various passive voltage probe bandwidth.

than 0.1 ns for bandwidth above 200 MHz, which is different to (12) but the difference is even higher with commonly used 0.35 constant value.

Conclusion

The bandwidth and rise time product has been derived for the generated square signal. The proposed analysis demonstrates differences between the commonly used band-width and rise time relation for a single inertia system. The article presents theoretical aspects of switching transistors and the frequency demands for measurement probes. Bandwidth requirements for switching power transistors are divided into two categories. The first focuses on the rising/falling slope, and the second addresses parasitic elements ringing in the power loop. The presented theory may provide a useful guideline for select-ing measurement equipment for converters. The presented results for system bandwidth highlight issues when the probe and oscilloscope have similar bandwidths. All theoretical aspects of required bandwidth were confirmed with practical measurements on a GaN-based commercial power board.

APPENDIX

Measuring high-speed analog signals, such as the drain-source voltage of SiC or GaN transistors, presents unique challenges due to the high switching speeds, high voltages, and potentially noisy environments. Below are the rule of thumb for requirements to perform high speed analog measurements:

1. **High-Bandwidth Probes and Oscilloscopes**

The measurement system must have a bandwidth much higher than the signal's switching frequency. For SiC or GaN transistors, which often switch in the MHz range with nanosecond-scale rise/fall times, a system bandwidth above equation (9) is typically required (best option is a system bandwidth as high as possible). Use a digital storage oscilloscope (DSO) with sufficient sampling rates (at least 5–10×the bandwidth) for accurate waveform capture with low-capacitance.

2. **Isolation and Safety**

High-voltage differential or isolated current probes are necessary for safety and to prevent ground loops, especially in high-side measurements. The best bandwidth range can be found on current shunt resistor and passible voltage probe. There are optical isolated volage probe which can be use with good bandwidth or pulse current transformer.

3. **Noise Immunity**

Minimize Ground Loops – use differential measurement techniques and proper grounding. Coaxial cables or shielded measurement setups should be use to reduce electromagnetic interference (EMI). Use low-pass filters to reduce high-frequency noise if it does not interfere with the desired measurement frequency range.

4. **High dV/dt Measurement Capability**

SiC and GaN transistors exhibit extremely fast switching with high dV/dt. Ensure the measurement system have a low input capacitance to handle fast transients an dhigh common-mode rejection ratio (CMRR) to differentiate signal from noise.

5. **Precision and Accuracy**

Regularly calibrate probes and the oscilloscope to maintain accuracy. The oscilloscope should have a wide dynamic range to capture both small and large voltage variations without distortion. Use oscilloscopes with high vertical resolution or mode. Ensure probes are properly compensated to match the oscilloscope's input.

6. **Thermal and Power Considerations**

High-speed measurements may induce heating in the circuit or probes; ensure thermal stability. Properly decouple power supply voltages near the transistor to avoid spurious oscillations. If analyzing switching waveforms in a circuit, synchronize measurements with the switching signals. Use appropriate trigger settings to capture fast transitions accurately.

Abbreviations

- BW – Bandwidth,
- DUT – Device under tests,
- DSO – Digital storage oscilloscope,
- FET – Field effect transistor,
- GaN – Gallium Nitride,
- ISE – Integral of the Square of the Error,
- Si – Silicon,
- SiC – Silicon Carbide,
- WBG – Wide-bandgap.

***Author**: Maciej Chojowski Ph.D., The AGH University of Krakow (AGH University), The Department of Power Electronics And Energy Control Systems , al. Adama Mickiewicza 30, 30–059 Kraków, E-mail: chojo@agh.edu.pl*

LITERATURA

[1] Palmer P., Zhang X., Shelton E., Zhang T., Zhang J., An experimental comparison of GaN, SiC and Si switching power devices, IECON 2017 – 43rd Annual Conference of the IEEE Industrial Electronics Society, Beijing, China, (2017), pp. 780–785, doi: 10.1109/IECON.2017.8216135.

[2] Al-bayati A. M. S., Alharbi S. S., Alharbi S. S., Matin M., A comparative design and performance study of a non-isolated DC-DC buck converter based on Si-MOSFET/Si-Diode, SiC-JFET/SiC-schottky diode, and GaN-transistor/SiC-Schottky diode power devices, 2017 North American Power Symposium (NAPS), Morgantown, WV, USA, (2017), pp. 1–6, doi: 10.1109/NAPS.2017.8107192.

[3] Millán J., Godignon P., Perpiñà X., Pérez-Tomás A., Rebollo J., A Survey of Wide Bandgap Power Semiconductor Devices, in IEEE Transactions on Power Electronics, vol. 29, no. 5, pp. 2155–2163, (2014), doi: 10.1109/TPEL.2013.2268900.

[4] Chen K. J., Häberlen O., Lidow A., Tsai C., Ueda T., Uemoto Y., Wu Y., GaN-on-Si Power Technology: Devices and Applications, in IEEE Transactions on Electron Devices, vol. 64, no. 3, pp. 779–795, (2017), doi: 10.1109/TED.2017.2657579.

[5] Wu Y., Jacob-Mitos M., Moore M. L., Heikman S., A 97.8% Efficient GaN HEMT Boost Converter With 300-W Out-put Power at 1 MHz, in IEEE Electron Device Letters, vol. 29, no. 8, pp. 824–826, (2008), doi: 10.1109/LED.2008.2000921.

[6] Rabkowski J., Peftitsis D., Nee H. P., Silicon Carbide Power Transistors: A New Era in Power Electronics Is Initiat-ed, in IEEE Industrial Electronics Magazine, vol. 6, no. 2, pp. 17–26, (2012), doi: 10.1109/MIE.2012.2193291.

[7] Weimer J., Kallfass I., Soft-Switching Losses in GaN and SiC Power Transistors Based on New Calorimetric Meas-urements, 2019 31st International Symposium on Power Semiconductor Devices and ICs (ISPSD), Shanghai, Chi-na, (2019), pp. 455–458, doi: 10.1109/ISPSD.2019.8757650.

[8] Chojowski, Baszyński M., Sosnowski R., Dziadecki A., High-Frequency Current Transformers Cascade for Power Electronics Measurements, Sensors 22, no. 15: 5846, (2022). https://doi.org/10.3390/s22155846.

[9] Ren Y., Xu M., Zhou J., Lee F. C., Analytical loss model of power MOSFET, in IEEE Transactions on Power Elec-tronics, vol. 21, no. 2, pp. 310–319, (2006), doi: 10.1109/TPEL.2005.869743.

[10] Ikeda N., Niiyama Y., Kambayashi H., Sato Y., Nomura T., Kato S., Yoshida S., GaN Power Transistors on Si Sub-strates for Switching Applications, in Proceedings of the IEEE, vol. 98, no. 7, pp. 1151–1161, (2010), doi: 10.1109/JPROC.2009.2034397.

[11] Rodríguez M., Zhang Y., Maksimović D., High-Frequency PWM Buck Converters Using GaN-on-SiC HEMTs, in IEEE Transactions on Power Electronics, vol. 29, no. 5, pp. 2462–2473, (2014), doi: 10.1109/TPEL.2013.2279212.

[12] Liu Z., Lee F. C., Li Q., Yang Y., Design of GaN-Based MHz Totem-Pole PFC Rectifier, in IEEE Journal of Emerging and Selected Topics in Power Electronics, vol. 4, no. 3, pp. 799–807, (2016), doi: 10.1109/JESTPE.2016.2571299.

[13] Azpúrua M. A., Pous M., Silva F., Uncertainty Analysis in the Measurement of Switching Losses in GaN FETs Power Converters, 2020 IEEE International Instrumentation and Measurement Technology Conference (I2MTC), Dubrovnik, Croatia, (2020), pp. 1–6, doi: 10.1109/I2MTC43012.2020.9129552.

[14] Zhang Z., Guo B., Wang F. F., Jones E. A., Tolbert L. M., Blalock B. J., Methodology for Wide Band-Gap Device Dy-namic Characterization, in IEEE Transactions on Power Electronics, vol. 32, no. 12, pp. 9307–9318, (2017), doi: 10.1109/TPEL.2017.2655491.

[15] Zhen C., Characterization and modeling of high-switching-speed behavior of SiC active devices, M.S. thesis, Dept. Elect. Eng., Virginia Polytech. Inst. State Univ., Blacksburg, VA, USA, (2009).

[16] Laimer G., KolarJ., Accurate Measurement of the Switching Losses of Ultra High Switching Speed CoolMOS Power Transistor/SiC Diode Combination Employed in Unity Power Factor PWM Rectifier Systems, Proceedings of the 8th European Power Quality Conference, Nuremberg, Germany, pp. 71–78, (2001).

[17] Chojowski M., Dziadecki A., Baszyński M., Dudek R., Stobiecki A., Skotniczny J., Wide Bandwidth and Inexpen-sive Current Sensor for Power Electronics – An Augmented LEM Current Sensor, Energies 14, no. 14: 4194, (2021). https://doi.org/10.3390/en14144194.

[18] Nitzsche M., Zehelein M., Troester N., Roth-Stielow J., Precise Voltage Measurement for Power Electronics with High Switching Frequencies, PCIM Europe 2018; International Exhibition and Conference for Power Electronics, Intelligent Motion, Renewable Energy and Energy Management, Nuremberg, Germany, (2018).

[19] Witcher J. B., Methodology for Switching Characterization of Power Devices and Modules. Master of Science thesis. Virginia Polytechnic Institute and State University, 2003–01–29.

[20] Zu G., Wen H., Zhu Y., Zhong R., Bu Q., Liu W., Zhao Y., Cui M., Review of Pulse Test Setup for the Switching Characterization of GaN Power Devices, in IEEE Transactions on Electron Devices, vol. 69, no. 6, (2022), doi: 10.1109/TED.2022.3168238.

[21] Li H., Gao Z., Chen R., Wang F., Improved Double Pulse Test for Accurate Dynamic Characterization of Medium Voltage SiC Devices, in IEEE Transactions on Power Electronics, vol. 38, no. 2, pp. 1779–1790, (2023), doi: 10.1109/TPEL.2022.3210749.

[22] Wang J., Yuan X., Rasekh N., Triple Pulse Test (TPT) for Characterizing Power Loss in Magnetic Components in Analogous to Double Pulse Test (DPT) for Power Electronics Devices, IECON 2020 The 46th Annual Conference of the IEEE Industrial Electronics Society, Singapore, (2020), pp. 4717–4724, doi: 10.1109/IECON43393.2020.9255039.

[23] Ma W., Wu Y., Li H., Chu D., Investigation of the Gate Resistance and the RC snubbers on the EMI Suppression in Applying of the SiC MOSFET, 2019 IEEE International Conference on Mechatronics and Automation (ICMA), Tian-jin, (2019), pp. 2224–2228, doi: 10.1109/ICMA.2019.8816376.

[24] Wu Y., Yin S., Li H., Ma W., Impact of RC Snubber on Switching Oscillation Damping of SiC MOSFET With Analyt-ical Model, in IEEE Journal of Emerging and Selected Topics in Power Electronics, vol. 8, no. 1, pp. 163–178, (2020), doi: 10.1109/JESTPE.2019.2953272.

[25] GaN Systems, GS66508B 650V Enhancement Mode GaN Transistor, GS66508B datasheet, (2020) [Rev 200402].

[26] Tektronix, Inc. MDO3000 Mixed Domain Oscilloscope. Available online: https://www.tek.com/oscilloscope/mdo3000-mixed-domain--oscilloscope (accessed on 03 March 2024).

[27] Tektronix, Inc. TPP1000 Passive Voltage Probes. Available online: https://www.tek.com/datasheet/passive-voltage-probes (accessed on 03 March 2024).